

Masses of Quasars



Bradley M. Peterson
The Ohio State University

“Fifty Years of Quasars”

9 September 2013

Measuring Central Black-Hole Masses: Direct vs. Indirect Methods

- *Direct methods*: based on dynamics of gas or stars accelerated by the central black hole.
 - Stellar dynamics, gas dynamics, reverberation mapping
- *Indirect methods*: based on observables correlated with the mass of the central black hole.
 - $M_{\text{BH}}-\sigma_*$ and $M_{\text{BH}}-L_{\text{bulge}}$ relationships, fundamental plane, AGN scaling relationships ($R_{\text{BLR}}-L$)

Primary and Secondary Methods

- Depends on model-dependent assumptions required.
- Fewer assumptions, little model dependence:
 - Proper motions/radial velocities of stars and megamasers (Sgr A*, NGC 4258)
- More assumptions, more model dependence:
 - Stellar dynamics, gas dynamics, reverberation mapping
 - Since the reverberation mass scale currently depends on other “primary direct” methods for a zero point, it is currently technically a “secondary method” though it is a “direct method.”
 - It will soon become a primary method.

Early Mass Estimates: The Eddington Limit

$$\frac{L\sigma_e}{4\pi r^2 c} < \frac{GMm}{r^2}$$

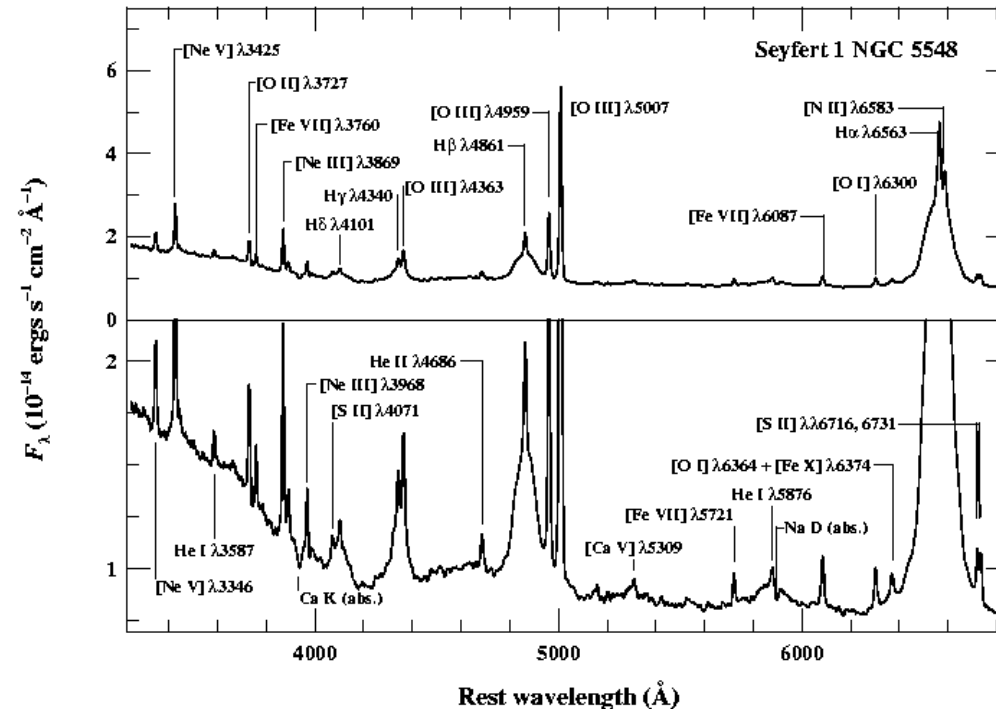
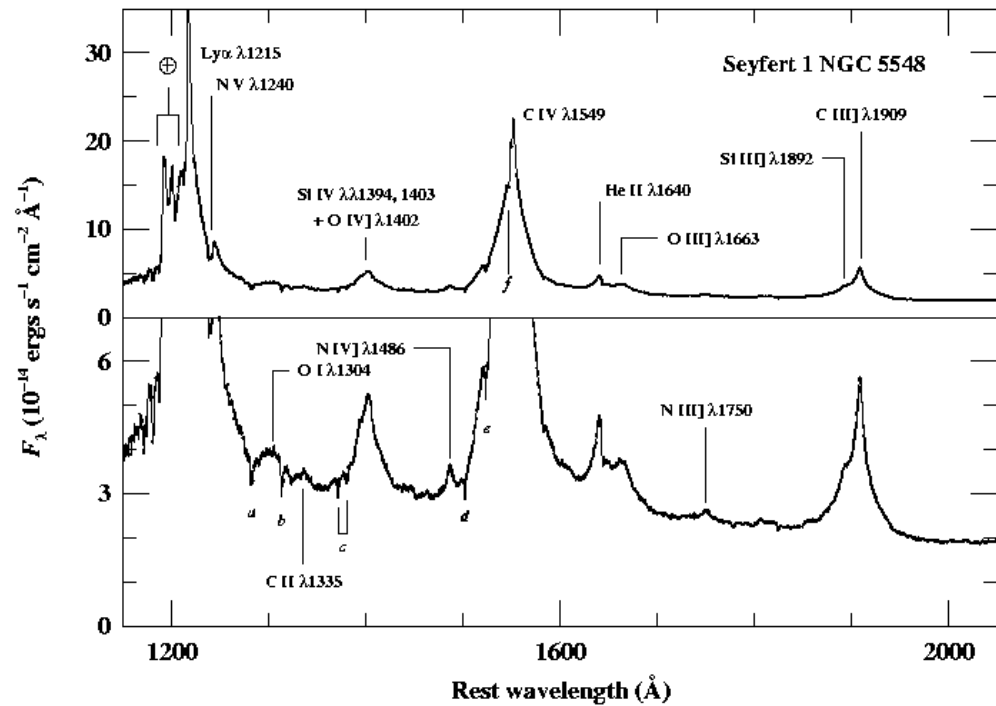
$$L < \frac{4\pi Gcm}{\sigma_e} M \approx 1.26 \times 10^{38} \left(\frac{M}{M_\odot} \right) \text{ergs s}^{-1}$$

- Outward radiation pressure cannot exceed gravity.

$$L \sim 10^{45} \text{ erg s}^{-1} \Rightarrow M > 10^7 M_\odot$$

The Broad-Line Region

- $1000 \leq \text{FWHM} \leq 25,000 \text{ km s}^{-1} \Rightarrow$ motion in deep potential?
 - $M \sim r \Delta V^2 / G$
- Spectra \Rightarrow Photoionized gas at $T \approx 10^4 \text{ K}$
- Absence of forbidden lines implies high density
 - But C III] $\lambda 1909 \Rightarrow n_e < 10^{10} \text{ cm}^{-3}$



The (Dimensionless) Ionization Parameter U

Rate at which H-ionizing photons are emitted by source.

$$Q_{\text{ion}}(H) = \int_{\nu_{\text{ion}}}^{\infty} \frac{L_{\nu}}{h\nu} d\nu$$

Ratio of ionizing photon density at distance r from source to particle density.

$$U = \frac{Q_{\text{ion}}(H)}{4\pi r^2 c n_{\text{H}}}$$

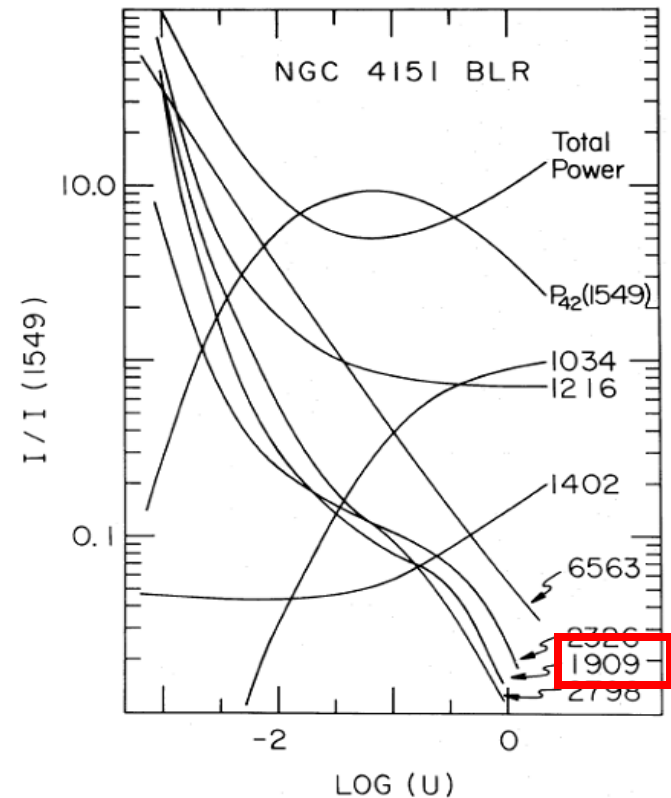
Aside:

$$r = \left[\frac{Q_{\text{ion}}}{4\pi U c n_{\text{H}}} \right]^{1/2} \propto L^{1/2}$$

Davidson 1972

Photoionization Model of the BLR in NGC 4151

- Single-cloud model cannot simultaneously fit low and high-ionization lines.
- Energy budget problem: line luminosities require more than 100% of the continuum energy.
- Single-cloud models predict size of BLR of order light year in bright Seyfert galaxies.

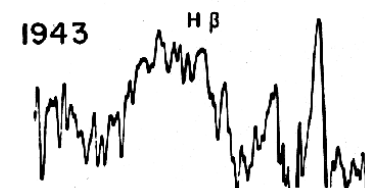
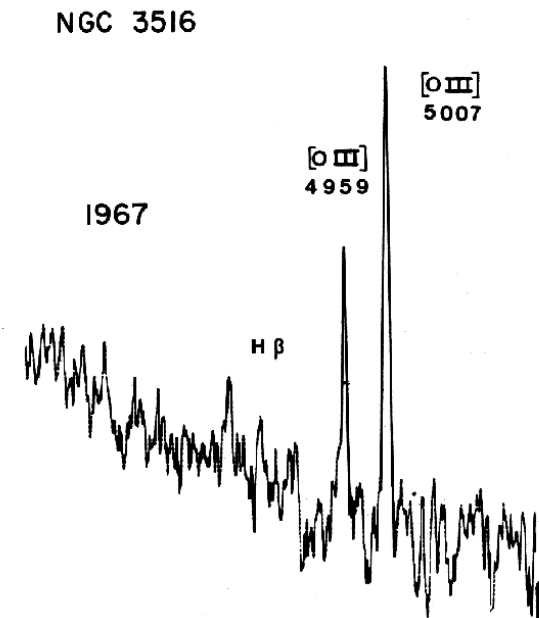
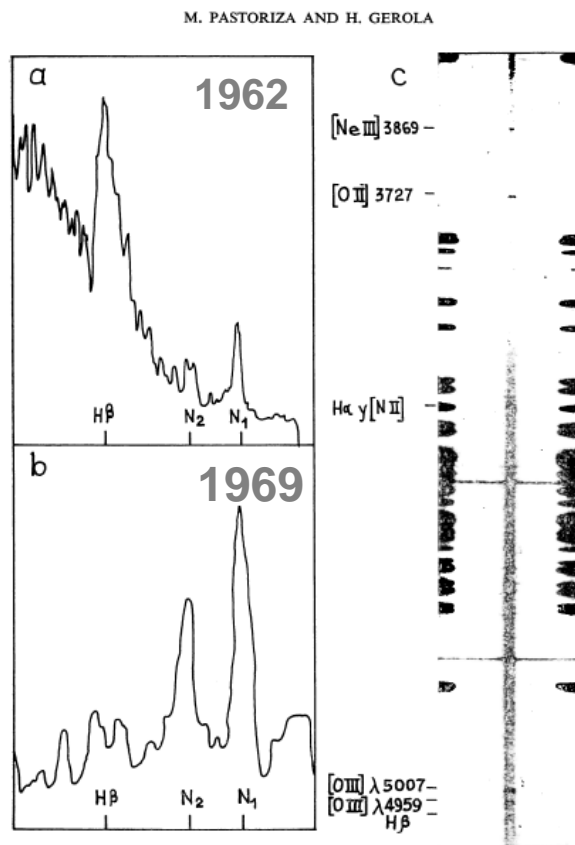


Ferland & Mushotzky 1982

Emission-Line Variability in Seyfert 1s

- First detected reported by Andrillat & Souffrin (1968) in NGC 3516
- Second case (NGC 1566) found by Pastoriza & Gerola (1970)

Photographic spectra reveal only extreme changes.



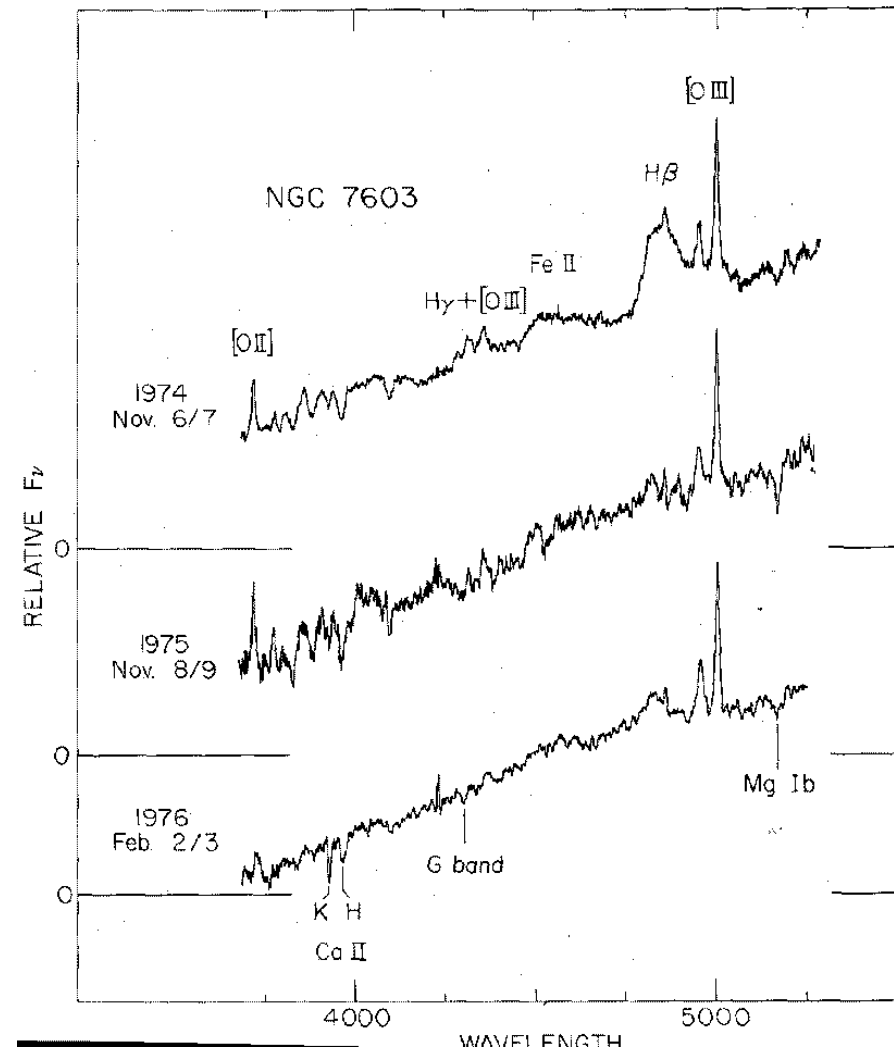
**Andrillat &
Souffrin 1968**

**Pastoriza &
Gerola 1970**

Emission-Line Variability

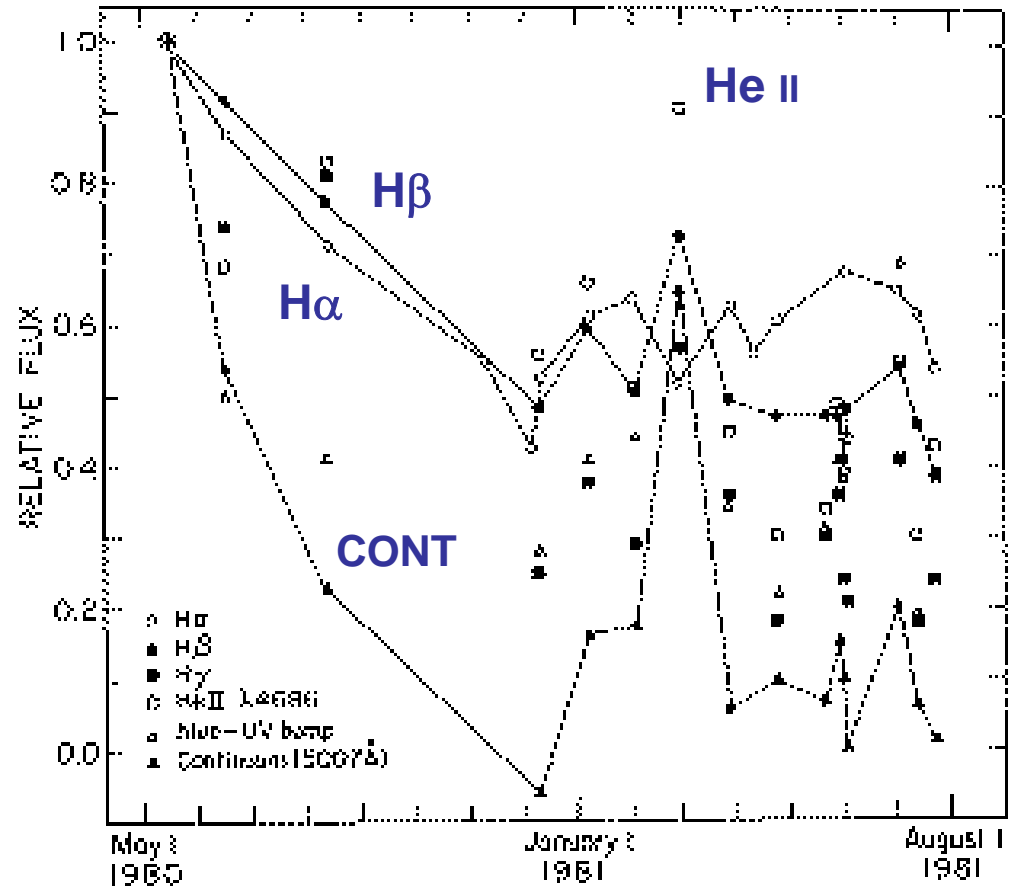
- Only very large changes could be detected photographically or with intensified television-type scanners (e.g., Image Dissector Scanners).
- Changes that were observed were often dramatic and reported as Seyferts “changing type” as broad components appeared or disappeared.

Tohline & Osterbrock 1976



First Monitoring Programs

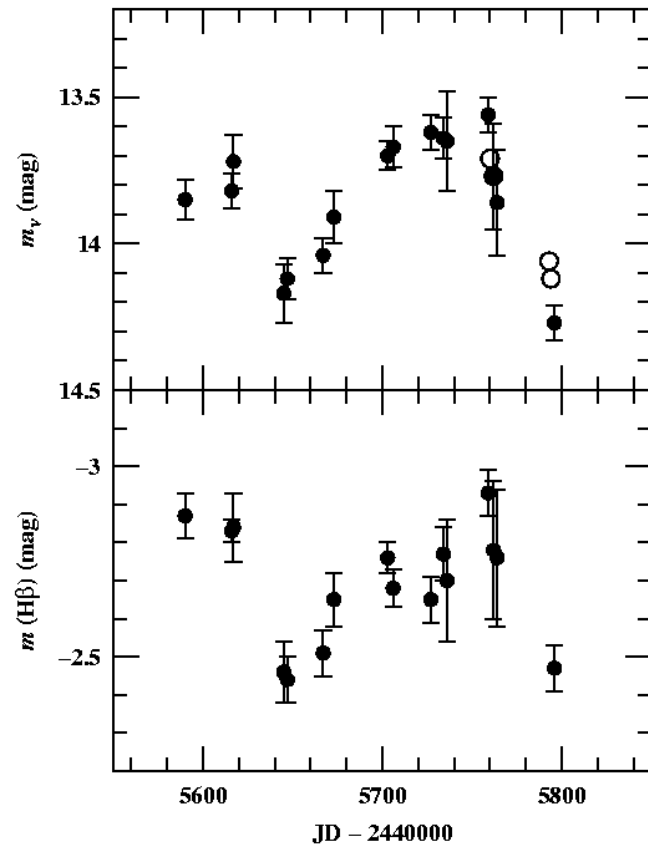
- NGC 4151:
 - Monitored at Lick Observatory by Antonucci and Cohen in 1980-81
 - short time scale response of Balmer lines (<1 month)
 - higher amplitude variability of higher-order Balmer lines and He II $\lambda 4686$



Antonucci & Cohen 1983

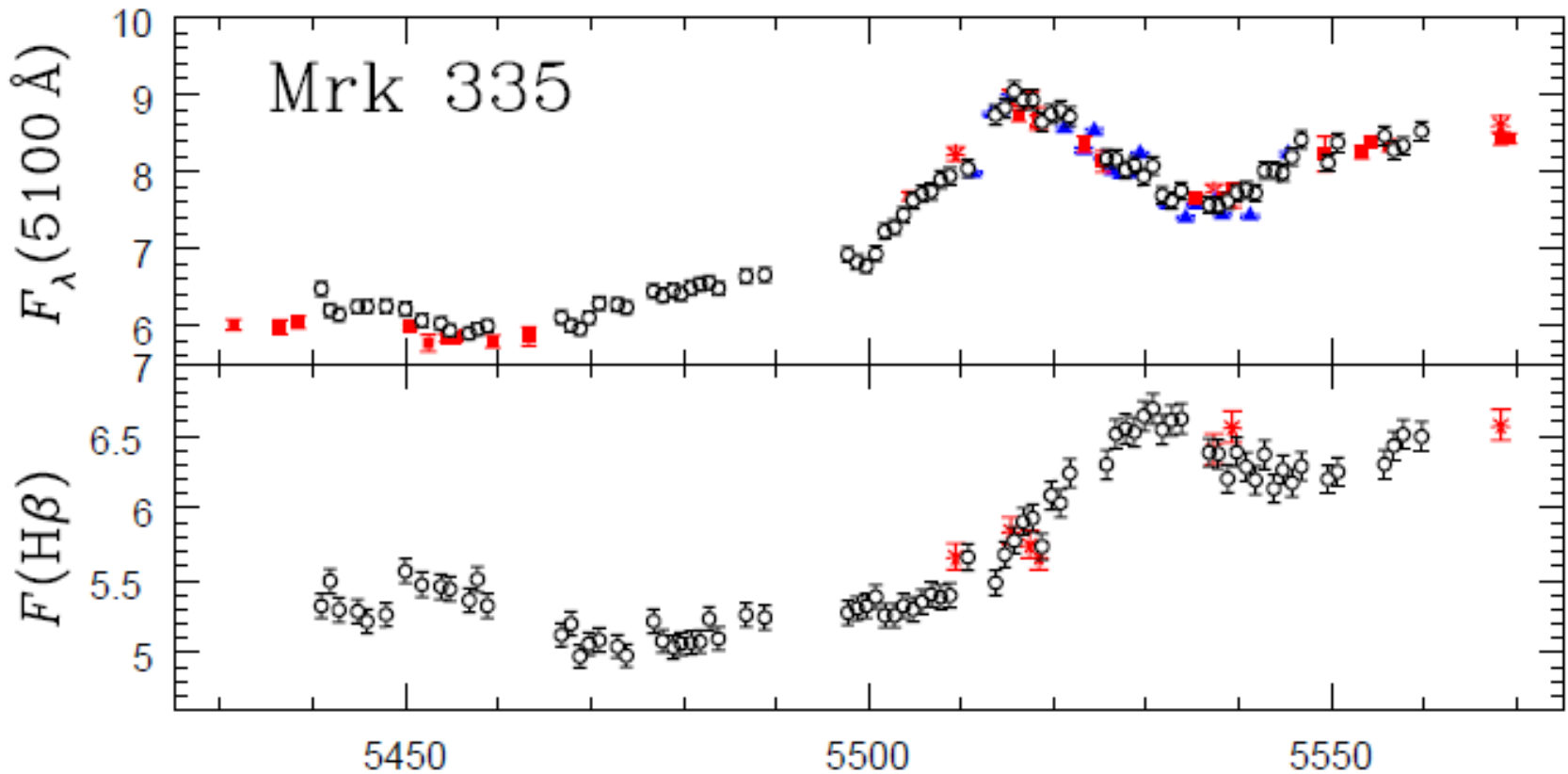
First Monitoring Programs

- Akn 120:
 - Monitored in optical by Peterson et al. (1983; 1985).
 - H β response time suggested BLR less than 1 light month across
 - Suggested serious problem with existing estimates of sizes of broad-line region
 - Higher luminosity source, so monthly sampling provided more critical challenge to BLR models



Data from Peterson et al. 1985

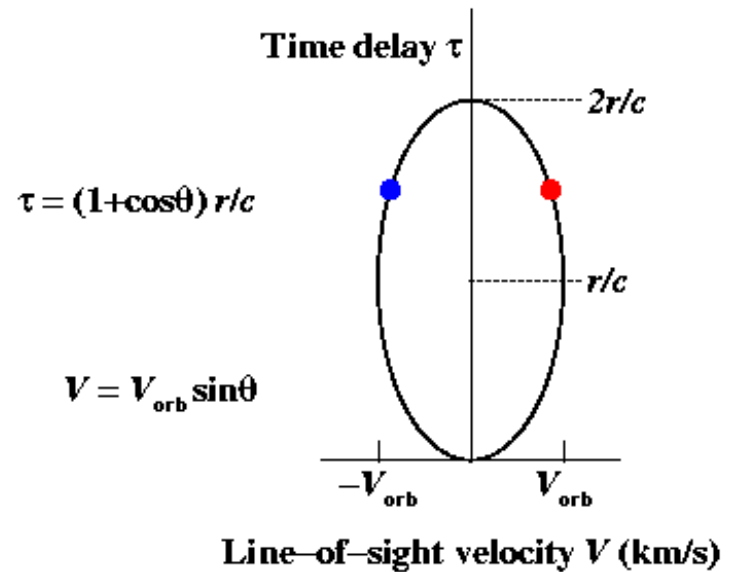
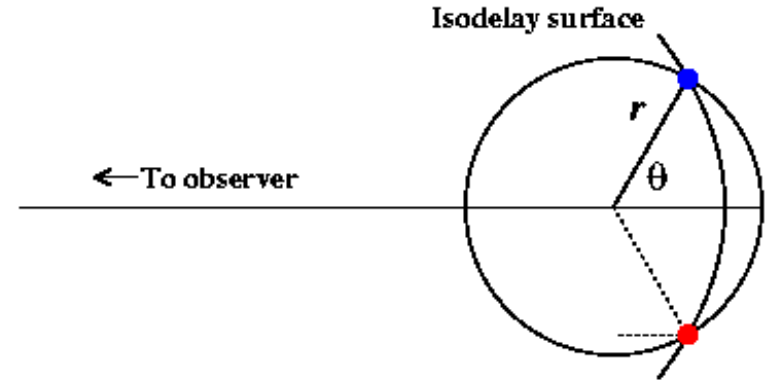
Reverberation Mapping



Emission line variations follow those in continuum with a small time delay (14 days here) due to light-travel time across the line emitting region.

Velocity-Delay Map for an Edge-On Ring

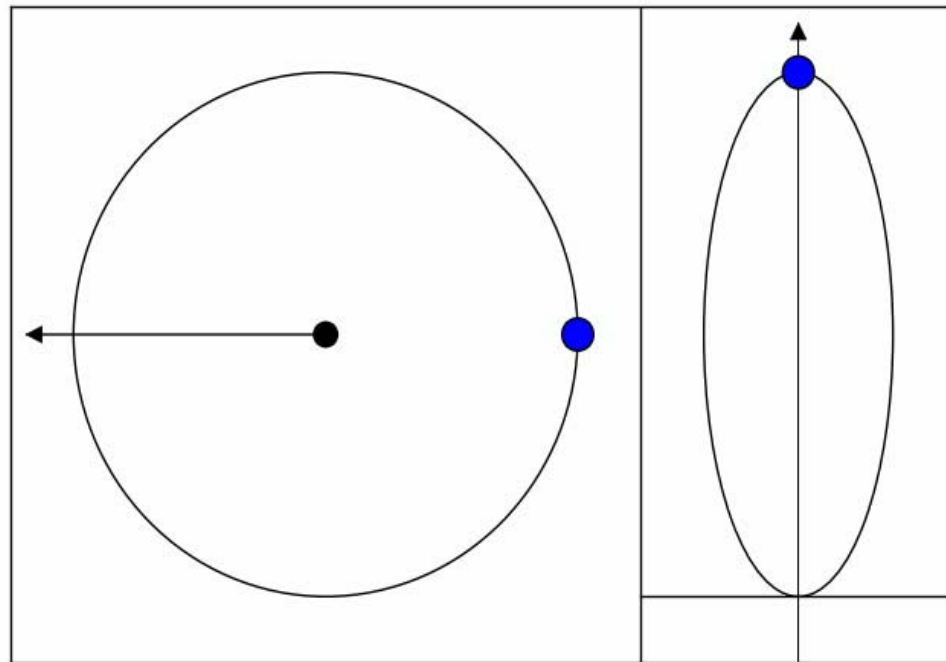
- Clouds at intersection of isodelay surface and orbit have line-of-sight velocities $V = \pm V_{\text{orb}} \sin \theta$.
- Response time is $\tau = (1 + \cos \theta)r/c$
- Circular orbit projects to an ellipse in the (V, τ) plane.



Velocity-Delay Map

Configuration space

Velocity-delay space



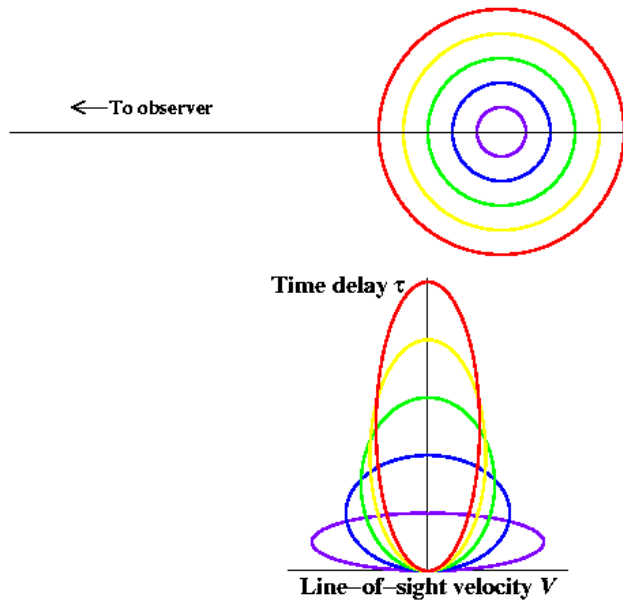
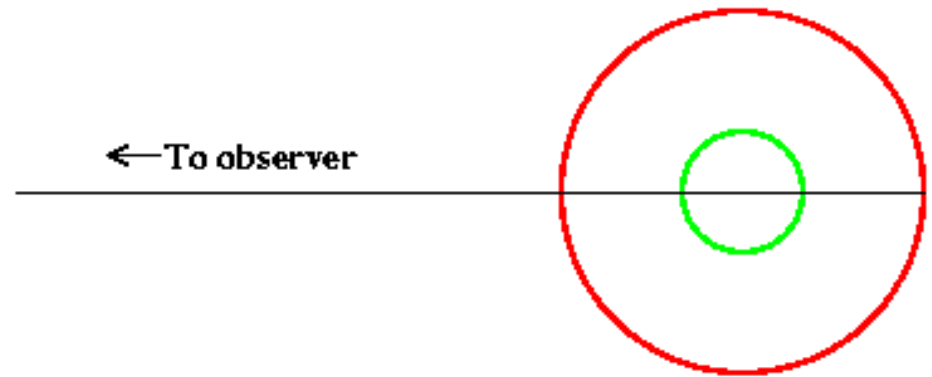
To observer

Time delay

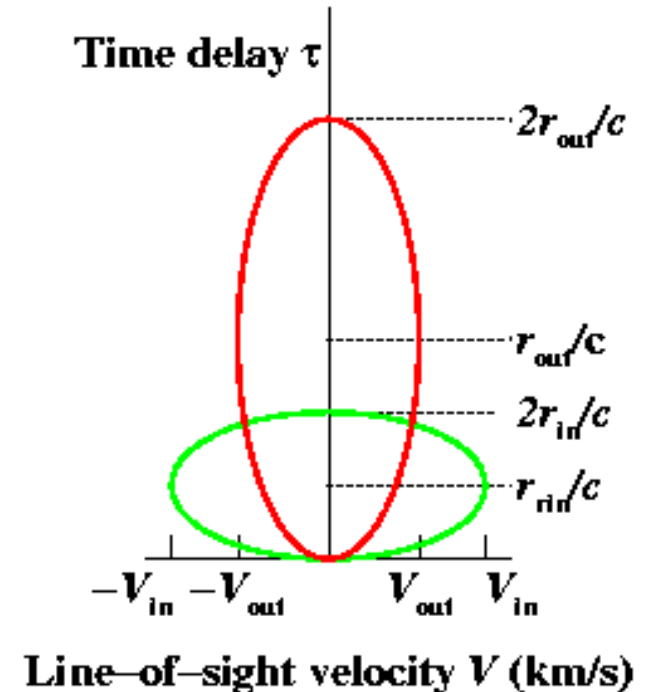
Doppler velocity

Thick Geometries

- Generalization to a disk or thick shell is trivial.
- General result is illustrated with simple two ring system.



A multiple-ring system



Time after continuum outburst

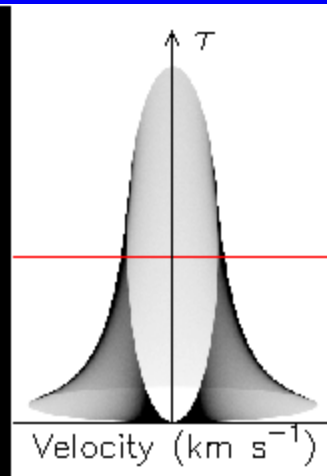
“Isodelay surface”

$$\tau = 18.6^d$$

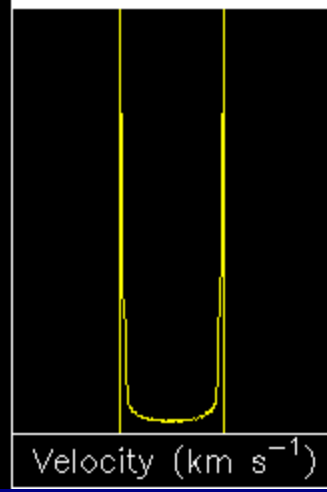
20 light days

**Broad-line region
as a disk,
2–20 light days**

Black hole/accretion disk



Time delay



Line profile at
current time delay

Reverberation Response of an Emission Line to a Variable Continuum

The relationship between the continuum and emission can be taken to be:

$$L(V, t) = \int \Psi(V, \tau) C(t - \tau) d\tau$$

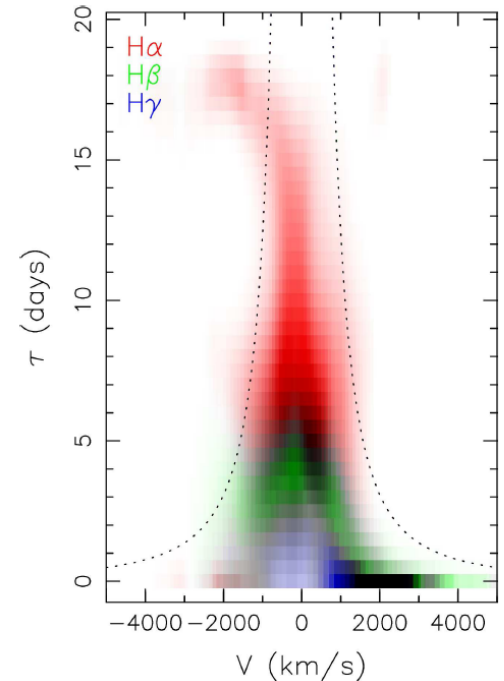
Velocity-resolved
emission-line
light curve

“Velocity-
delay map”

Continuum
light curve

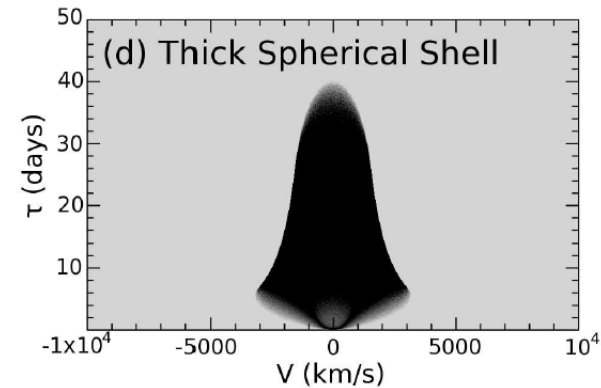
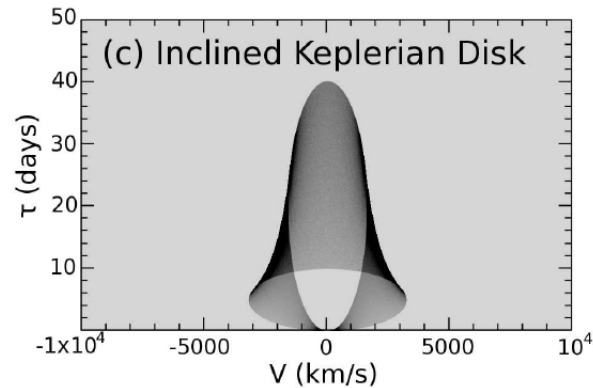
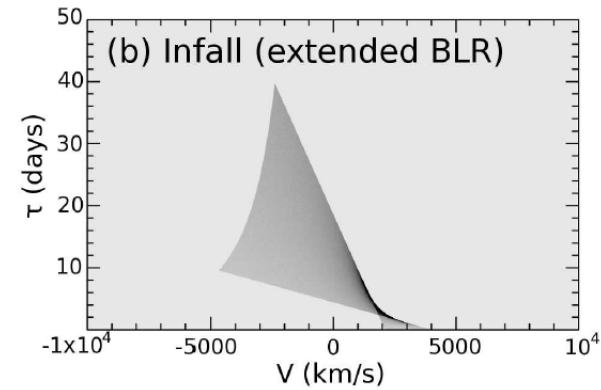
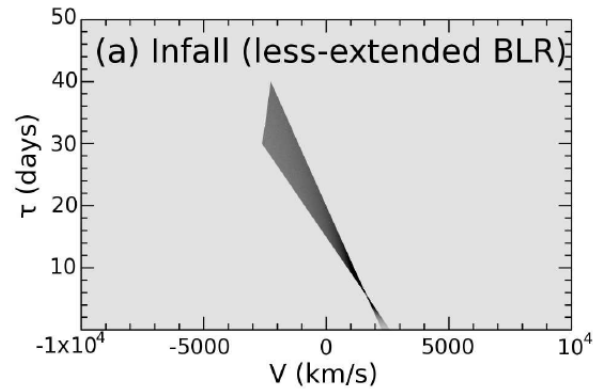
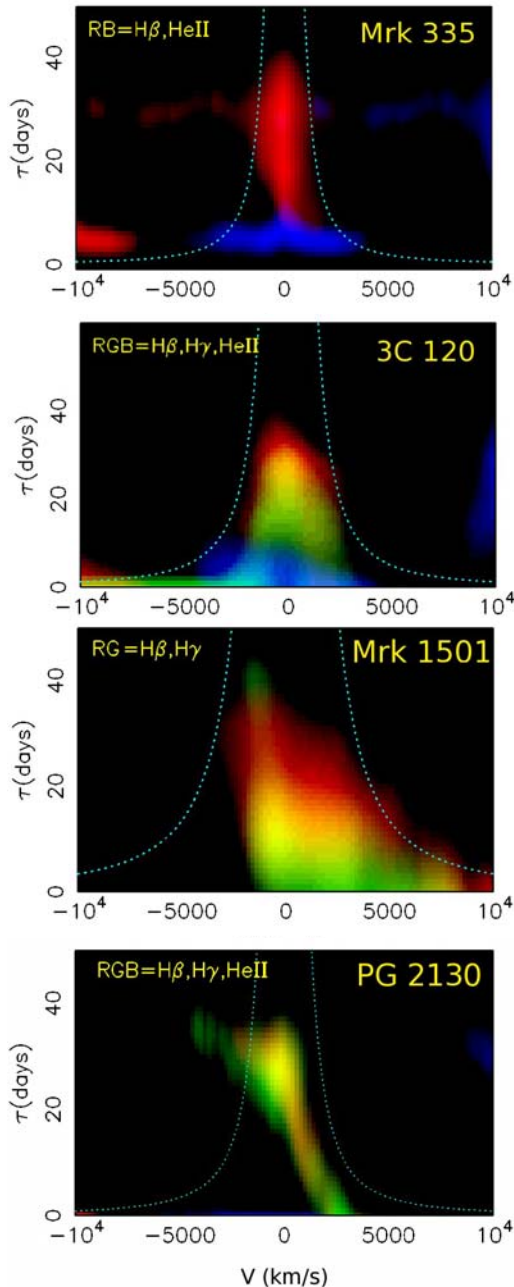
Velocity-delay map is observed line response to a δ -function outburst

Required time sampling, duration, and S/N makes velocity-delay map recovery very difficult.



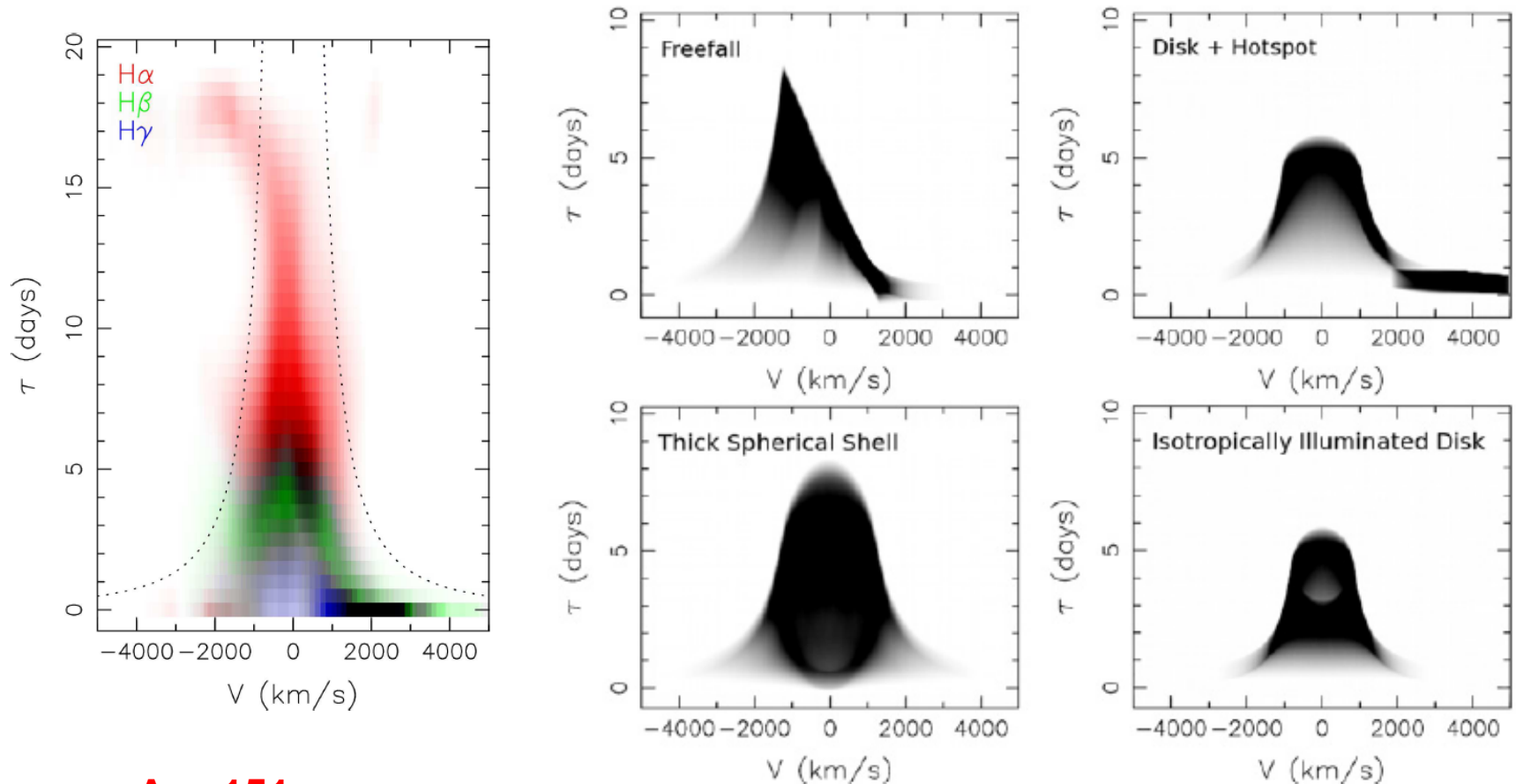
Arp 151
LAMP: Bentz+ 2010

Toy Models



Grier+ 2013, ApJ, 764:47

A Complex Multicomponent Broad-Line Region?

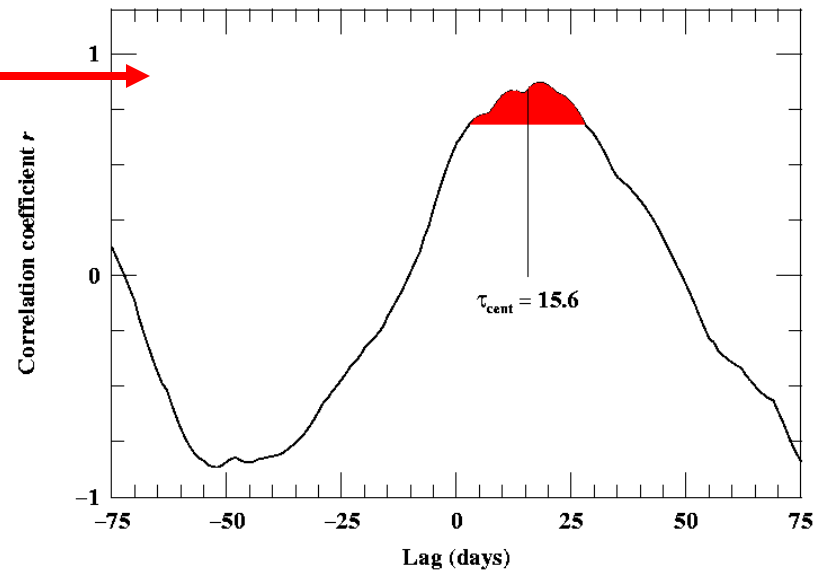
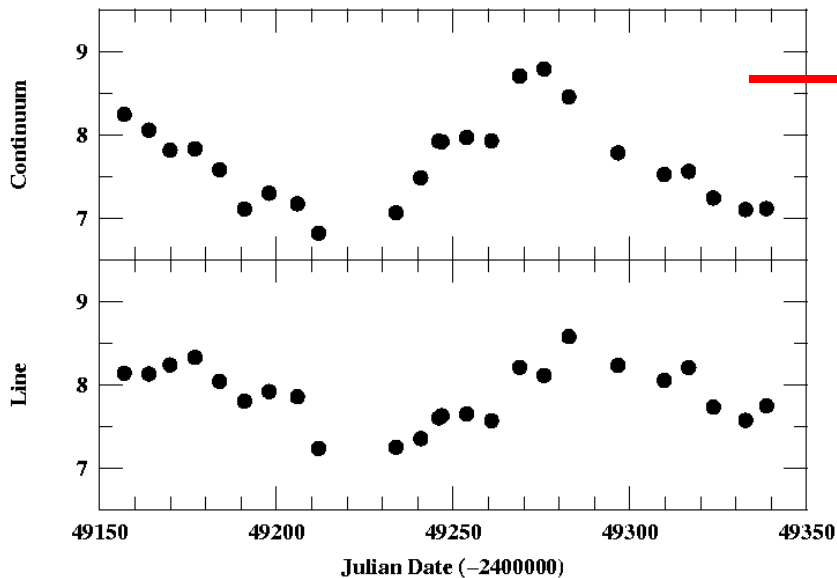


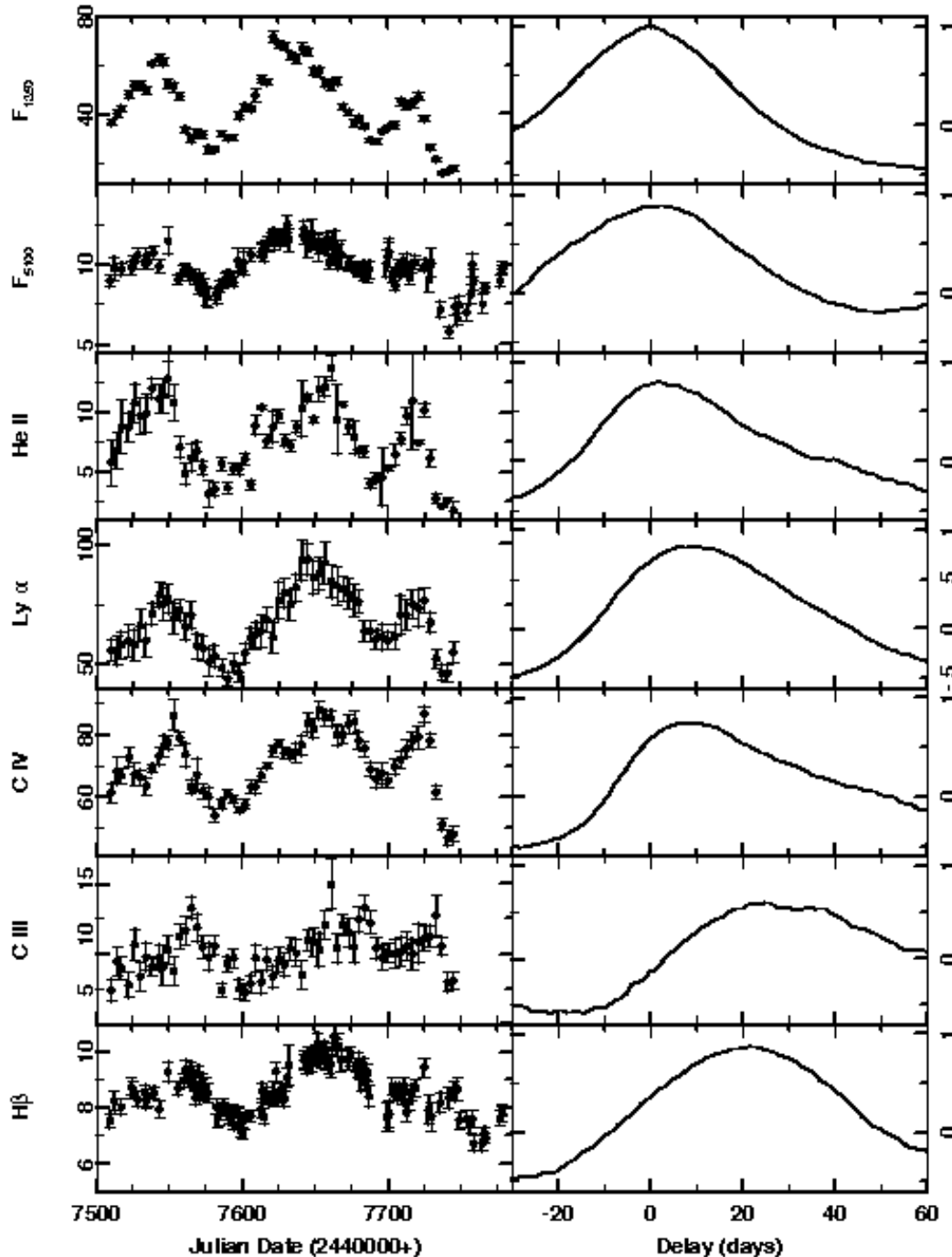
Arp 151
LAMP: Bentz+ 2010

Emission-Line Lags

- Because the data requirements are *relatively* modest, it is most common to determine the cross-correlation function and obtain the “lag” (mean response time):

$$\text{CCF}(\tau) = \int \Psi(\tau') \text{ACF}(\tau - \tau') d\tau'$$

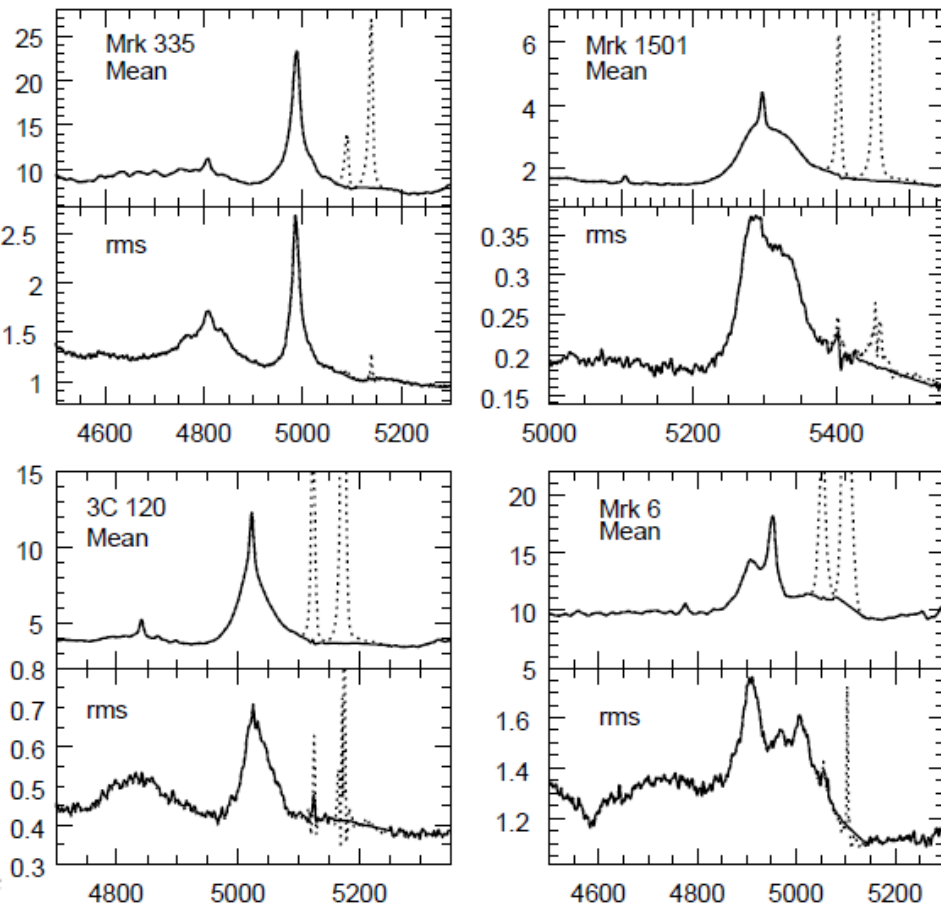




Reverberation Mapping Results

- Reverberation lags have been measured for ~ 50 AGNs, mostly for H β , but in some cases for multiple lines.
- AGNs with lags for multiple lines show that highest ionization emission lines respond most rapidly \Rightarrow ionization stratification

Measuring the Emission-Line Widths

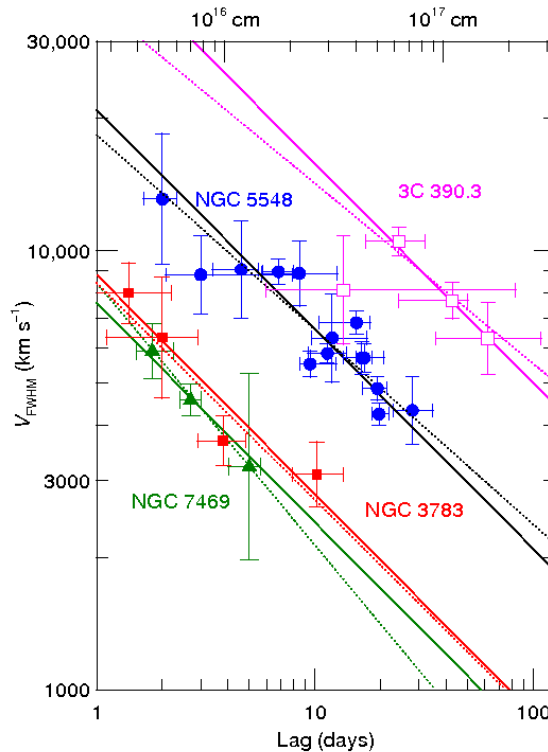


- We preferentially measure line widths in the rms residual spectrum.
 - Constant features disappear, less blending.
 - Captures the velocity dispersion of the gas that is responding to continuum variations.

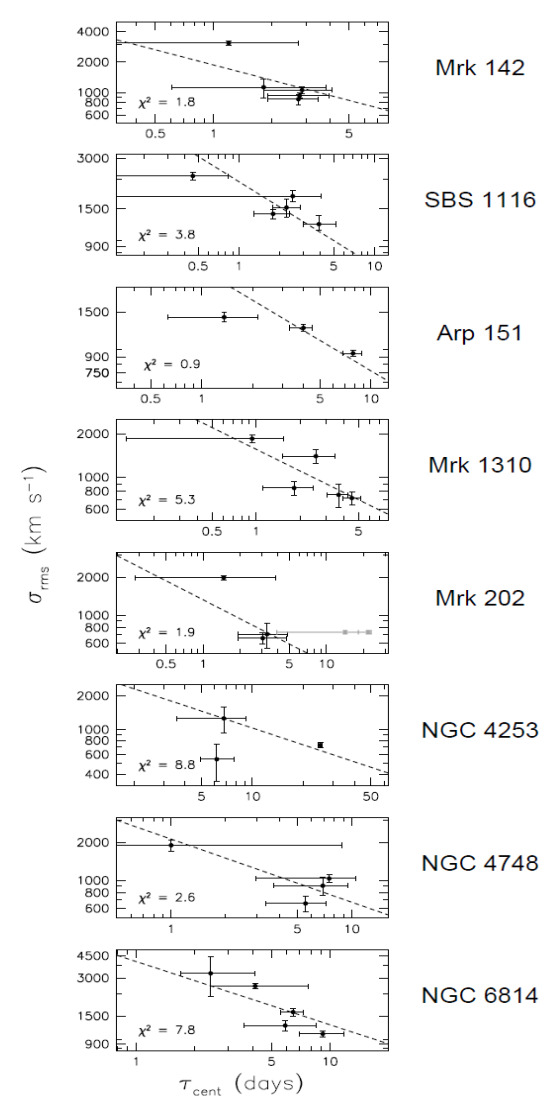
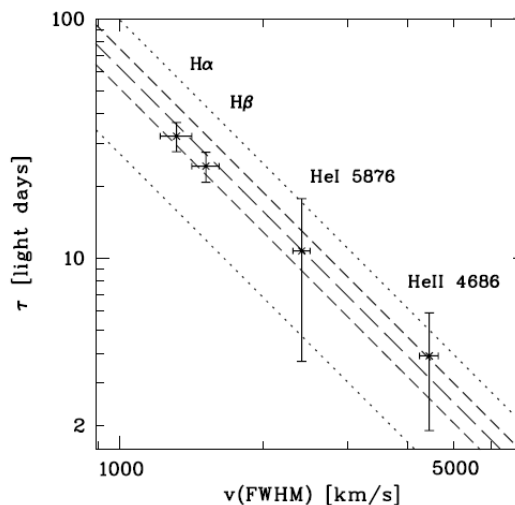
Grier+ 2012, ApJ, 755:60

A Virialized BLR

- $\Delta V \propto R^{-1/2}$ for every AGN in which it is testable.
- Suggests that gravity is the principal dynamical force in the BLR.
 - Caveat: radiation pressure!



Peterson & Wandel 2002



Bentz+ 2009

Kollatschny 2003

Reverberation-Based Masses

“Virial Product” (units of mass)

$$M_{\text{BH}} = f \frac{r \Delta V^2}{G}$$

Observables:

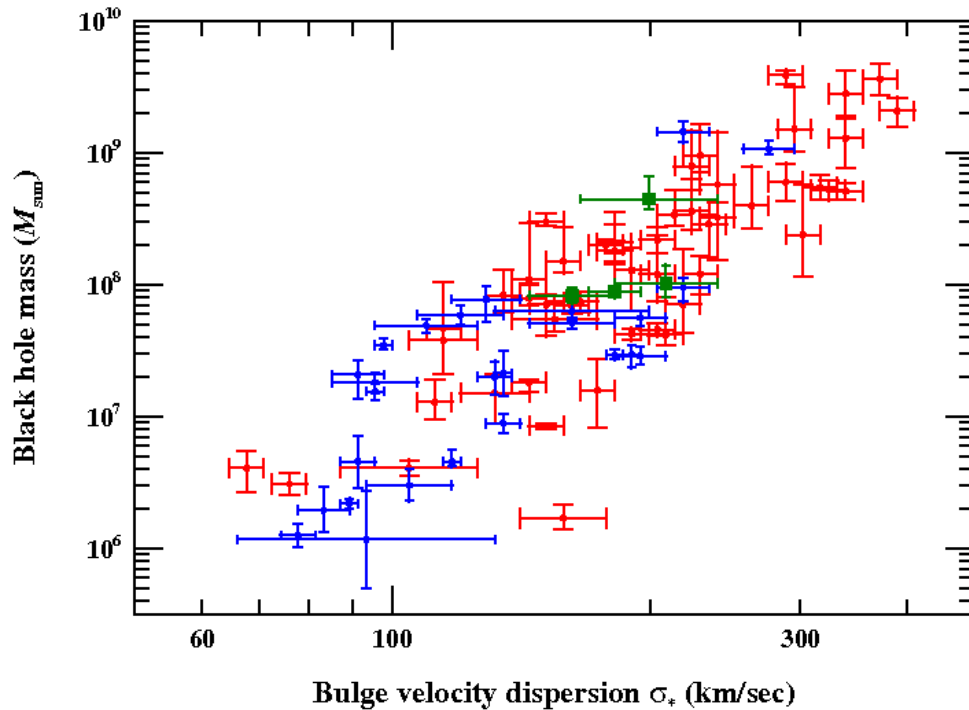
r = BLR radius (reverberation)

ΔV = Emission-line width

Set by geometry and inclination
(subsumes everything we don't know)

If we have independent measures of M_{BH} , we can compute an ensemble average $\langle f \rangle$

The AGN $M_{\text{BH}}-\sigma_*$ Relationship

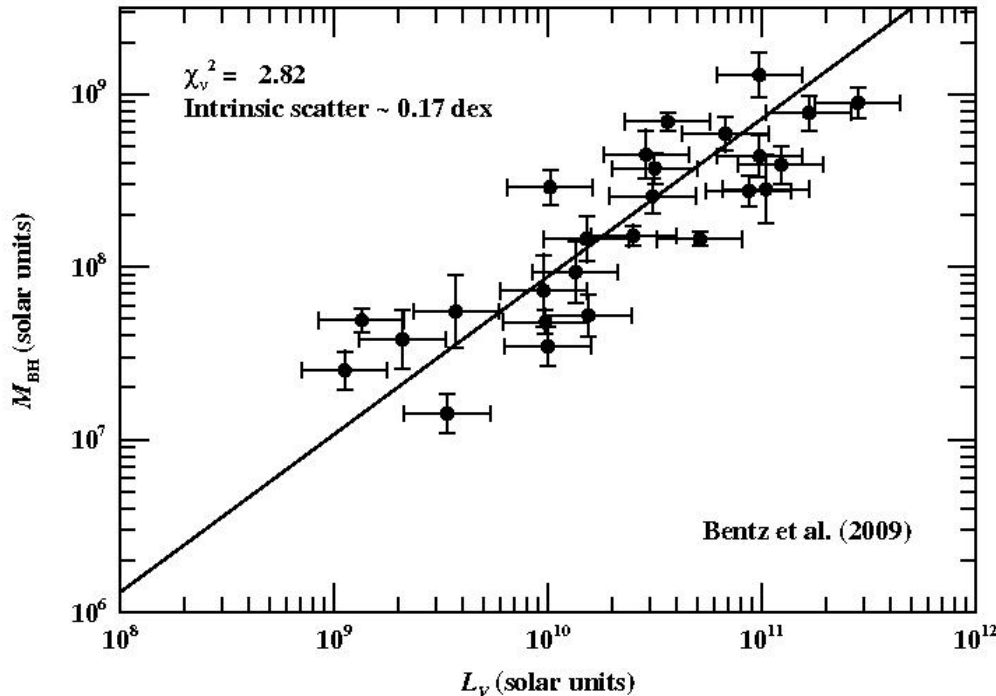


- AGN
- AGN, new H -band σ_*
- Quiescent galaxy

Grier+ 2013, ApJ, 773:90

- Assume zero point of most recent quiescent galaxy calibration.
 $\langle f \rangle = 4.19 \pm 1.08$
- Maximum likelihood places an upper limit on intrinsic scatter
 $\Delta \log M_{\text{BH}} \sim 0.40$ dex.
 - Consistent with quiescent galaxies.

The AGN $M_{\text{BH}}-L_{\text{bulge}}$ Relationship



- Line shows best-fit to quiescent galaxies
- Maximum likelihood gives upper limit to intrinsic scatter $\Delta \log M_{\text{BH}} \sim 0.17$ dex.
 - Smaller than quiescent galaxies ($\Delta \log M_{\text{BH}} \sim 0.38$ dex).

Black Hole Mass Measurements

(units of $10^6 M_{\odot}$)

Galaxy	NGC 4258	NGC 3227	NGC 4151
Direct methods:			
Megamasers	38.2 ± 0.1	N/A	N/A
Stellar dynamics	33 ± 2	7–20	$47^{+11}_{-14} \dagger$
Gas dynamics	25 – 260	20^{+10}_{-4}	$30^{+7.5}_{-22}$
Reverberation	N/A	7.63 ± 1.7	46 ± 5

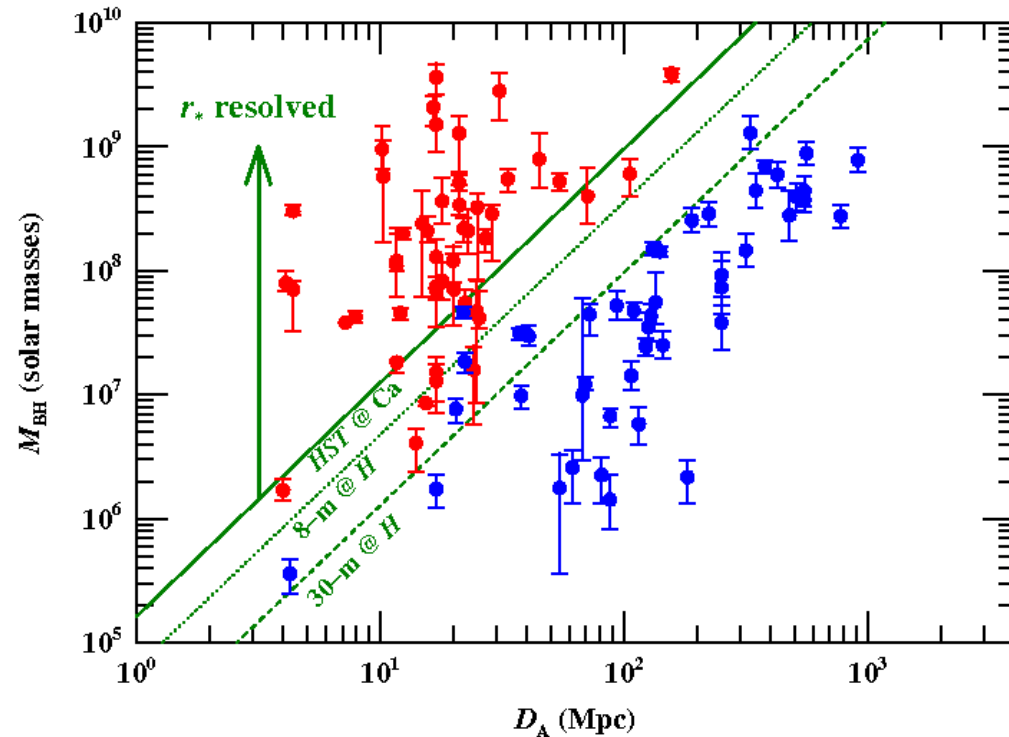
Quoted uncertainties are statistical only, not systematic.

References: see Peterson (2010) [arXiv:1001.3675]

† Onken et al., in preparation

Masses of Black Holes in Quasars

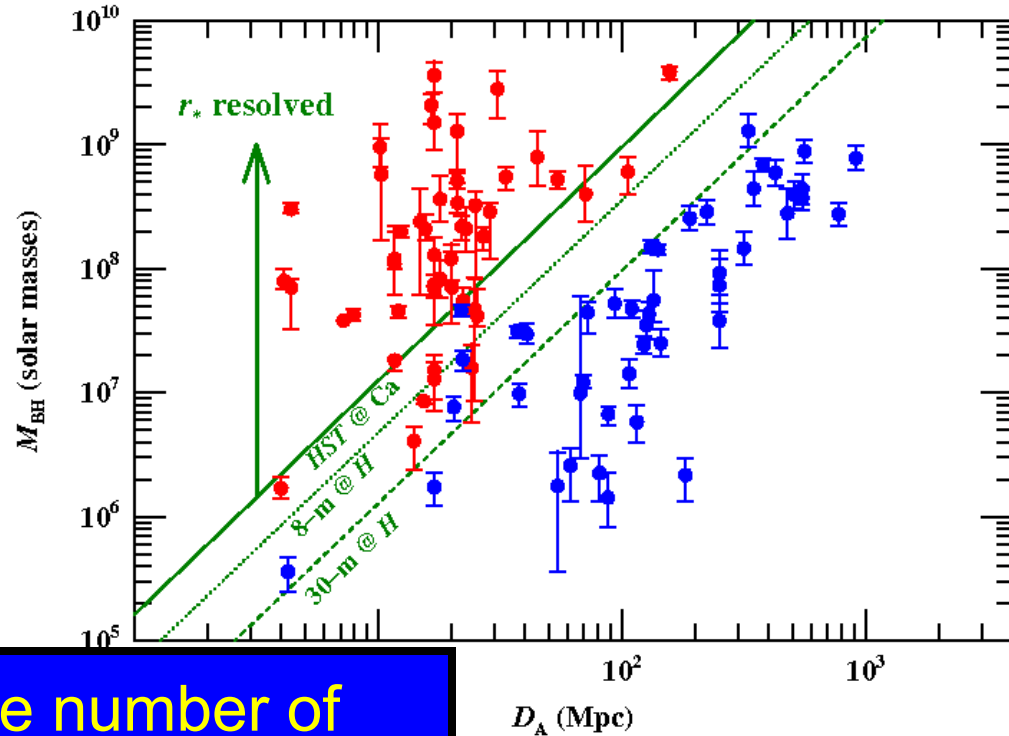
- Stellar and gas dynamics requires higher angular resolution to proceed further.
 - Even a 30-m telescope will not vastly expand the number of AGNs with a resolvable r_* .
- Reverberation is the future path for direct AGN black hole masses.
 - Trade time resolution for angular resolution.
 - Downside: resource intensive.



- Quiescent galaxies
- RM AGNs

Masses of Black Holes in Quasars

- Stellar and gas dynamics requires higher angular resolution to proceed further.
 - Even a 30-m telescope will not vastly expand the number of AGNs with a resolvable r_* .
- Reverberation is the future path for direct AGN black hole masses.
 - Trade time resolution for



To significantly increase number of measured masses, we need to go to secondary methods.

quiescent galaxies
AGNs



NGC 4051

$z = 0.00234$

$\log L_{\text{opt}} = 41.8$

Mrk 79

$z = 0.0222$

$\log L_{\text{opt}} = 43.7$

PG 0953+414

$z = 0.234$

$\log L_{\text{opt}} = 45.1$

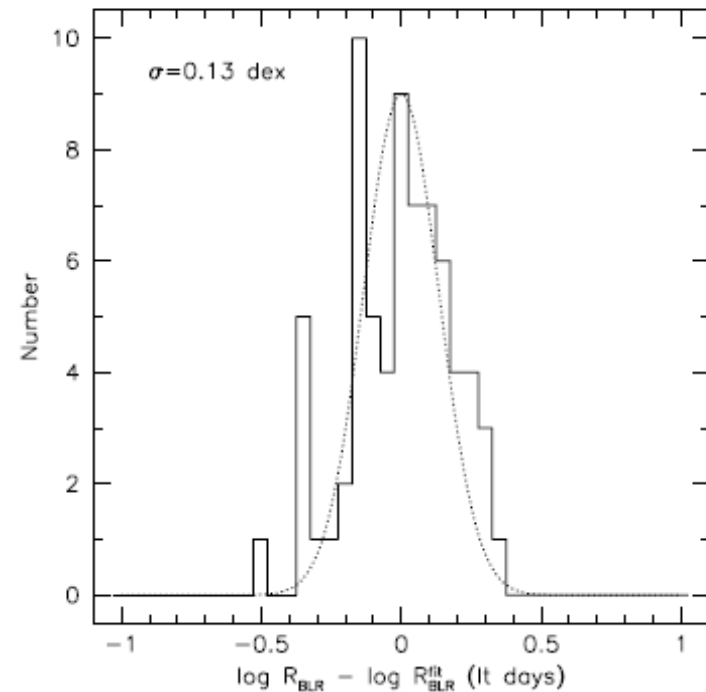
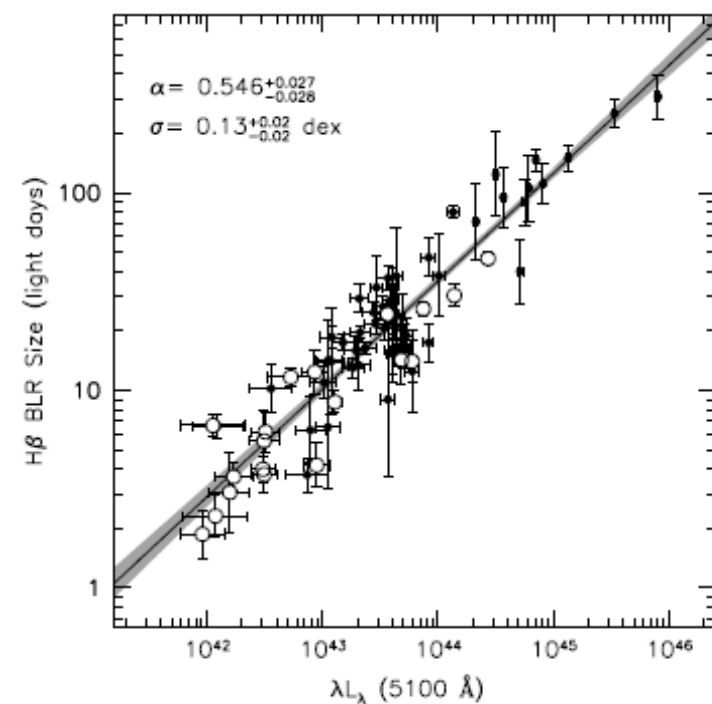
Reverberation experiments use large spectrograph apertures for accurate spectrophotometry.

This results in significant starlight contribution to the measured optical luminosity.

The $R-L$ Relation

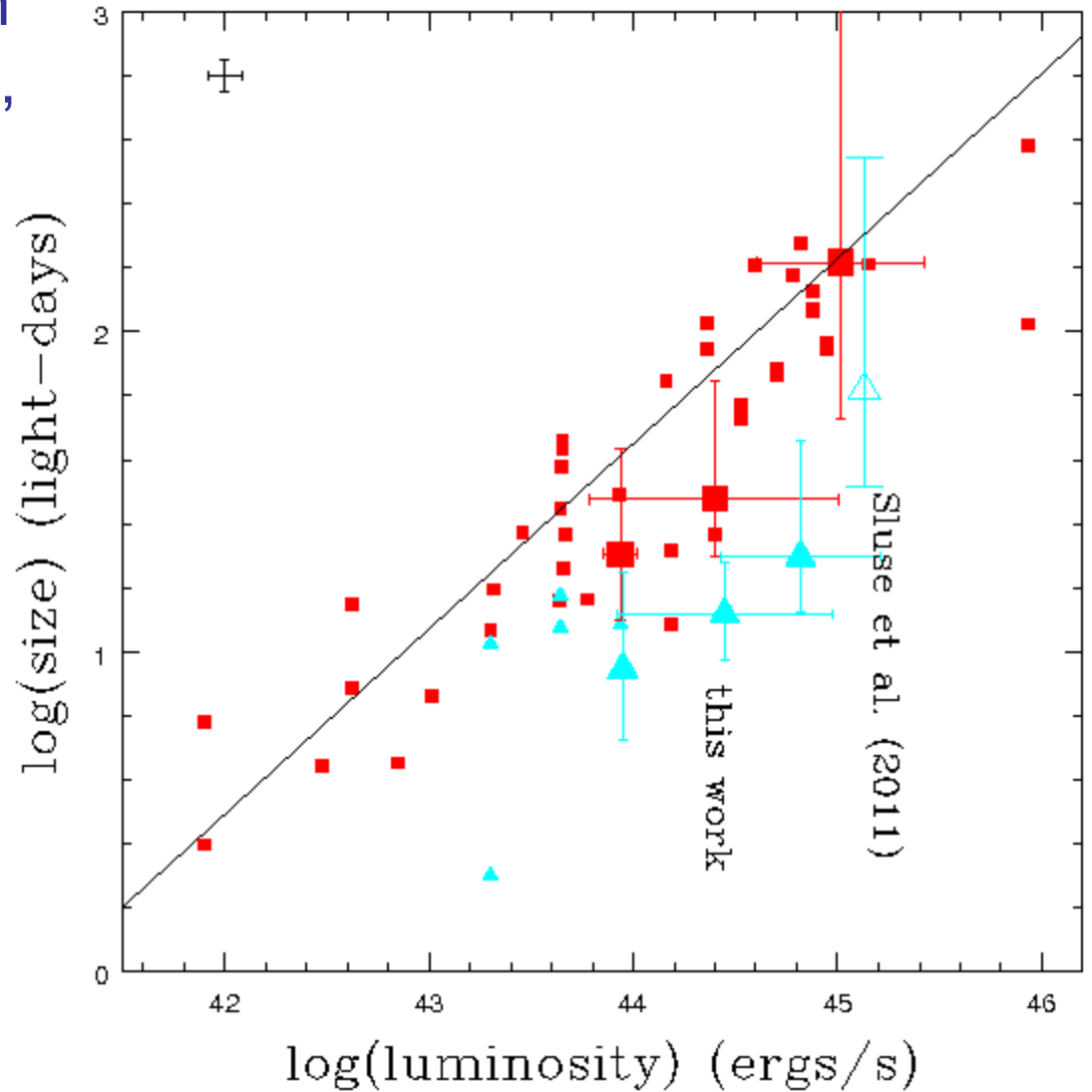
- Empirical slope $\sim 0.55 \pm 0.03$
- Intrinsic scatter ~ 0.13 dex
- Typical error bars on best reverberation data ~ 0.09 dex
- Conclusion: for $H\beta$ over the calibrated range ($41.5 \leq \log L_{5100} \text{ (ergs s}^{-1}\text{)} \leq 45$ at $z \approx 0$), $R-L$ is nearly as effective as reverberation.

Bentz+ 2013



Independent confirmation
of $R-L$ from microlensing,
including high-ionization
lines.

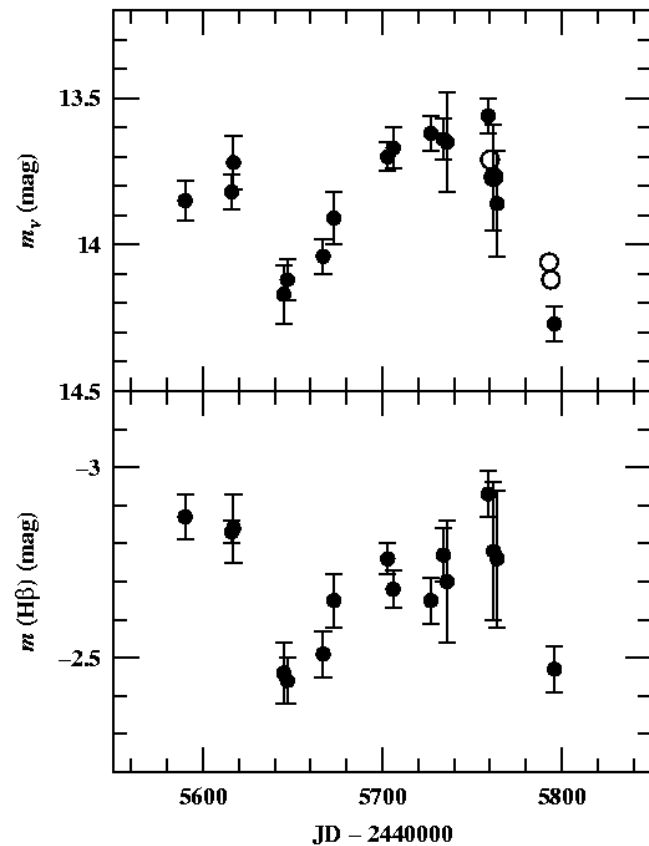
- RM measurements,
low ionization lines
- Microlensing,
Low-ionization lines
- RM measurements,
high-ionization lines
- Microlensing,
high-ionization lines



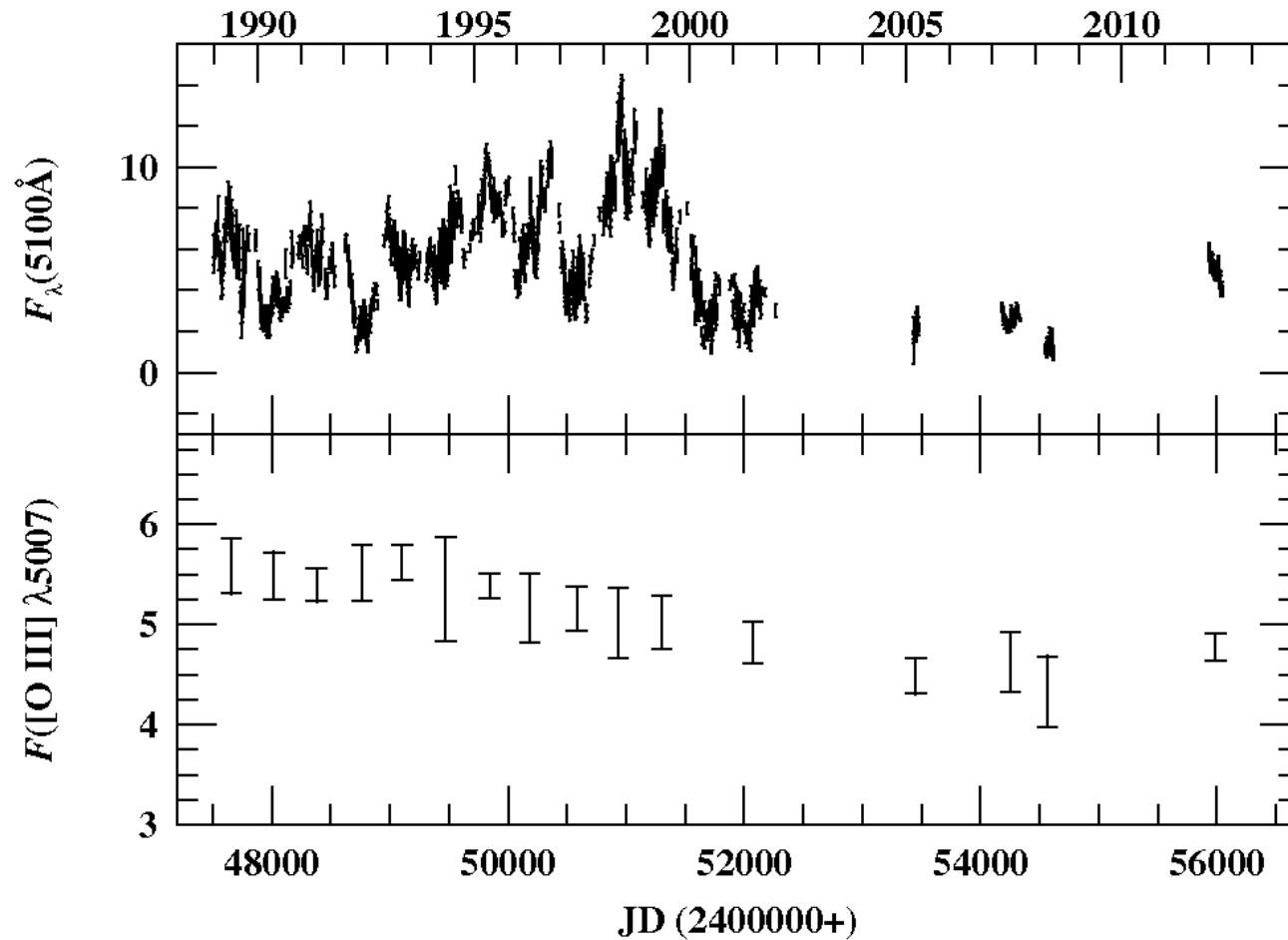
Guerras, Kochanek + 2013

And now for something completely different.

It's...



Narrow Emission-Line Variability in NGC 5548



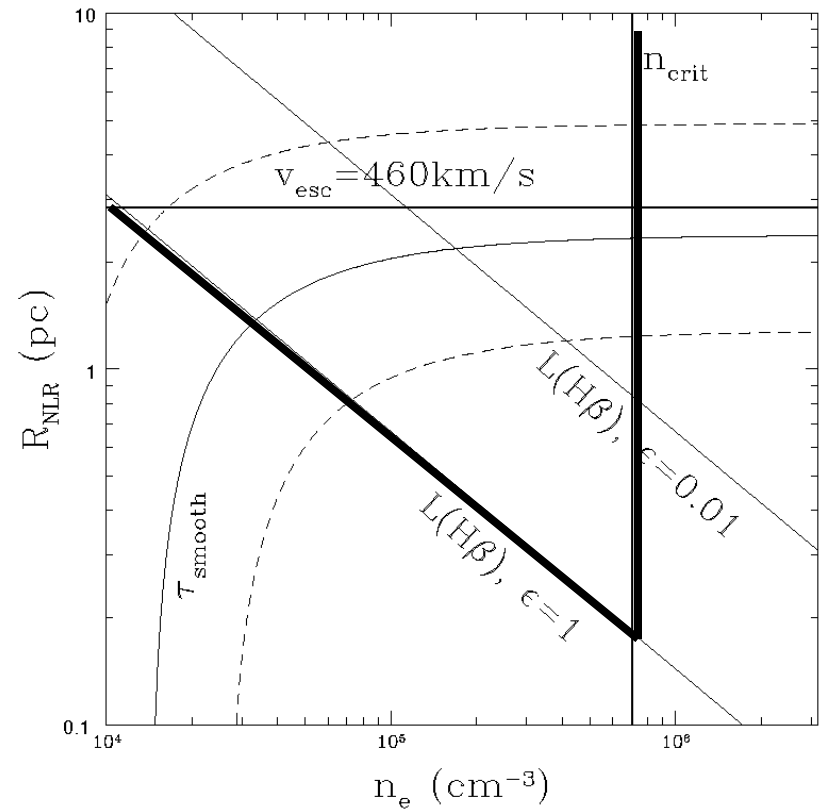
Peterson+, on astro-ph today

Narrow Emission-Line Variability in NGC 5548

$$\tau_{\text{smooth}} = \left(\frac{2R_{\text{NLR}}}{c} \right) + \left(\frac{1}{n_e \alpha_B} \right)$$

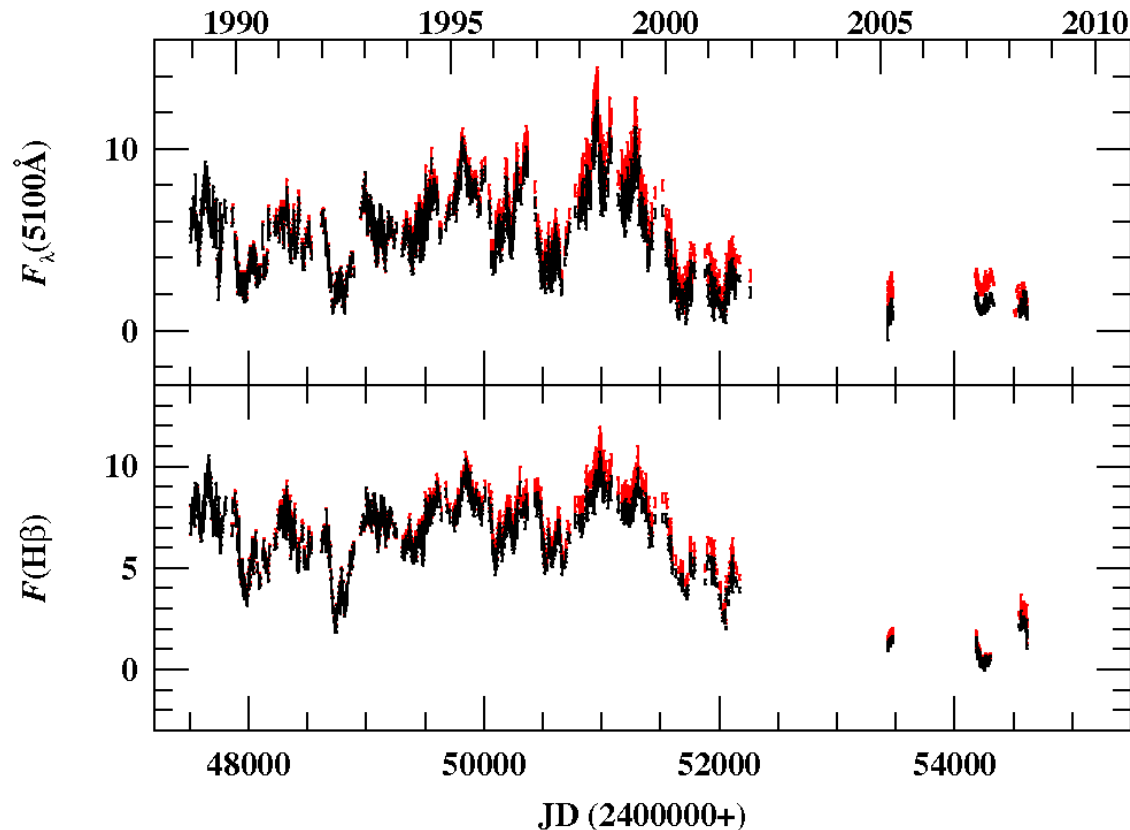
Light-travel time
Recombination timescale

- Size of narrow-line region constrained to 1-3 pc
- Density $\sim 10^5 \text{ cm}^{-3}$
- Second credible detection of [O III] variability (3C 390.3 by Zheng+ 1995), but first to measure R_{NLR}



Peterson+, on astro-ph today

Narrow Emission-Line Variability in NGC 5548



Requires recalibration of long-term light curves,
but doesn't affect any reverberation results to date.

To Conclude

- Reverberation mapping has reached a level of maturity:
 - BH masses becoming increasingly reliable, typically 0.3-0.4 dex over a range of more than 3 orders of magnitude
 - Beginning to probe BLR structure/kinematics
 - All maps so far show evidence for infall in the Balmer lines
 - We are preparing a new UV RM program (180 orbits) for execution in Cycle 21 with HST. Goal: first high-fidelity UV velocity-delay maps.
 - Techniques that can be applied on “industrial scales” are under development.